FOREX Publication
Open Access | Rapid and quality publishing

International Journal of
Electrical and Electronics Research (IJEER)
Research Article | Volume 12, Special Issue -BDF| Pages 19-27 | e-ISSN: 2347-470X

# Filtering based Image Decomposition and Restoration Approach

**Nilesh Singh V. Thakur[1], Saurabh A. Shah[2]**
[1]*Department of Computer Technology, Yeshwantrao Chavan College of Engineering, Nagpur, India, thakurnisvis@rediffmail.com*
[2]*Department of Computer Science and Engineering, Prof Ram Meghe College of Engineering and Management, Badnera, India, shahsaurabh.15@gmail.com*

*Correspondence: thakurnisvis@rediffmail.com

**ABSTRACT-** In image processing, most of the time it is required to process the image by partitioning or decomposing it in different parts or representing it by mean of different features. Also, the quality of an acquired or received image is very much important from the further processing point of view. The partitioning or decomposition of the image and reconstruction of the original image from the distorted image are the prime areas of research when deals with the image filtering. Presented research work deals with the decomposition of the distorted color image and the restoration of the original color image. Average filtering is used for the decomposition of each grey level planes of the image in three components and later, the average and median filters are used to reconstruct the color image from these decomposed components of each grey level planes. Different experiments are carried out with the insertion of 0.01 to 0.05 variance Gaussian white noise (GWN). The proposed approach is evaluated on the basis of identified performance evaluation parameters, *i.e.*, mean squared error; peak signal to noise ratio; signal to noise ratio; structural similarity index measure; and correlation coefficient. Presented image decomposition approach is lightweight from the implementation point of view and based on the obtained results, it is observed that the median filter produces the good result where small details are required in image restoration.

**General Terms:** Image processing; Image partitioning.
**Keywords:** Image decomposition; Image restoration; Image filtering.

**ARTICLE INFORMATION**
**Author(s)**: Nilesh Singh V. Thakur and Saurabh A. Shah;
**Received**: 04/09/2023; **Accepted**: 11/12/2023; **Published**: 28/03/2024;
**e-ISSN**: 2347-470X;
**Paper Id**: IJEER-BDF04;
**Citation:** 10.37391/ijeer.12bdf04
**Webpage-link**:
https://ijeer.forexjournal.co.in/archive/volume-12/ijeer-12bdf04.html

This article belongs to the Special Issue on **Innovations and Trends in Computer, Electrical, and Electronics Engineering: Bridging the Digital Frontier**



## 1. INTRODUCTION

The images are, in general, usually transmitted from one place to another through electronic gadgets due to the huge use of cameras and social network. Cameras and sensors are used for the image acquisition. Collected images may be of good quality or blurred due to the illumination effect or the noise. In literature, different approaches are reported to handle the noisy images. Now-a-days, huge image data transmission takes place on social media through the Internet and most of the data is associated with the images. So, it is necessary to have the good image restoration or denoising approach to handle the noisy images to preserve the quality of images. The main purpose of the presented research work is to explore different filtering techniques in view of the image decomposition and restoration. In general, filter banks are used for the image decomposition purpose. Presented work explores the average filter technique from the image decomposition point of view. Also, average and median filters are explored from the image restoration point of view. Here, the main aim is to develop light weight image decomposition approach using similar type of filter in view of image restoration. Image decomposition is generally used to represent the image from processing point of view. As per requirement of the problem domain, one can decompose the image into different parts or components. The image decomposition approach cannot be evaluated directly, rather, it can be evaluated with reference to the application of it. There is no widespread and standard description for the image decomposition evaluation parameters that can be used by researchers, rather it can be evaluated through the application of developed image decomposition approach. Here, the developed decomposition approach is used for the purpose of image restoration. In presented work, the obtained results are evaluated with respect to the image restoration performance evaluation parameters.

Different image decomposition approaches are reported in the literature which are based on the different type of filter banks. Huang et al. [1] identified image components based on the semantic similarity and the input image is advocated by the self-learning process directly. Cui et al. [2] developed dictionary learning based approach to decompose the artifacts in the high-frequency part of the Computed Tomography images. Du et al. [3] developed an approach which uses the decomposition method in multi-scale transform fusion for functional and structural information from the Positron Emission Tomography (PET) images and grey Magnetic Resonance Imaging (MRI). Hauagge et al. [4] modeled an image-space approach to estimate the ambient occlusion in the image set with varying unknown illumination. Kang et al. [5] designed an intrinsic image

FOREX Publication
Open Access | Rapid and quality publishing
International Journal of Electrical and Electronics Research (IJEER)
Research Article | Volume 12, Special Issue -BDF| Pages 19-27 | e-ISSN: 2347-470X

decomposition method for the classification of hyper spectral image. Jin and Gu [6] developed an intrinsic image decomposition approach for the hyperspectral images to decompose into reflectance and shading components. Kang et al. [7] designed the image decomposition-based image fusion approach. Ono et al. [8] developed an approach using texture characterization and image is decomposed into texture and cartoon components. Zhang and Patel [9] developed an approach where the texture and the cartoon type images are represented using a set of generic filters. Gupta and Singh [10] designed an image partitioning approach for removing texture as well as preservation of edges. Shao et al. [11] designed an edge-preserving image decomposition approach for preserving the edge retention, detail smoothening and shape fitting based on joint weighted least squares. Song et al. [12] developed an image decomposition approach for structure-conserving image decomposition. Jiang and Yin [13] developed a fractional order regularization operator for image decomposition. Huang and Wang [14] developed an effective texture-conserving image decomposition approach that is dependent on image decomposition. Bellamine and Tairi [15] developed a structure–texture image decomposition approach. Canh et al. [16] discussed a detail-conserving reconstruction approach based on residual renovation and cartoon texture. Qiang et al. [17] designed an image decomposition approach using the adaptive local Laplacian filter and image is decomposed into texture and structural element. Yang et al. [18] developed an approach where the image is decomposed into texture and edge components. Liu et al. [19] designed multi-focus image integration approach for overcoming the problems related to the morphological structures of multi-focus images. Jiang et al. [20] developed a nighttime image quality improvement approach dependent on image decomposition to improve visibility of the image. Zhang et al. [21] designed a local-to-global optimization approach for recovering illumination in the shadow portions of large outdoor scenarios. Ma et al. [22] developed a sparse high frequency gradient approach for image smoothening. Muhammad et al. [23] designed a hybrid watermarking method using wavelet with Arnold transform image decomposition and partial pivoting upper and lower triangular disintegration. Fan et al. [24] developed a tight frame-based group sparsity regularization for the decomposition. Ha et al. [25] designed an image decomposition model for simultaneous color matching. Chang and Chen [26] developed a fusion of transmission images and backscatter images based on multi-scale decomposition. Rong et al. [27] designed a sparse representation and hybrid image decomposition for image fusion. Jamlee Ludes and Norman [28] developed a total variation and image decomposition model for the extraction of cartoon-texture component. Thakur and Kakde [29] designed a mechanism to form a single grey plane image from three color plane images. Different filtering techniques are studied in Mahakale and Thakur [30]. Vedic mathematics is explored by Panchbhai and Thakur [31] in view of image filtering. Kamble et al. [32] discussed about the decomposition of video using automata theory and motion estimation to carry out fractal coding.

Presented research work deals with the development of the image-decomposition based restoration approach. The sole aim of this research work is associated with the development of the image decomposition approach to facilitate the image restoration. Average filter is used for the image decomposition to generate three components from the degraded grey level image. Later these obtained three components of the grey level plane are filtered through the average and median filter. The key significant contribution of the presented research is that the developed approach is light in implementation complexity and uses a similar type of filter with a good compromise of reconstructed image quality.

## 2. PROPOSED APPROACH

Presented work deals with the development of average-filter based image decomposition approach. This approach involves the insertion of noise and then the filtered images are integrated. This section describes the proposed filtering-based image decomposition and restoration approach. The proposed approach is, basically, applicable to the grey level images. This approach includes the degradation of the original grey or color image if the original image is not the noise affected image. If the original grey level image is not the noise affected then the noise is added to it and later, the decomposition starts. If the original image is the color image (e.g., RGB color space image), then the color image is degraded first (if it is not noise affected) by adding the noise and later, separating three grey level planes (R, G, and B) and then the proposed decomposition approach is applied on each plane from the decomposition point of view.

### 2.1 Image Degradation Model

If the original grey level image is not noise affected then it is degraded with the noise addition. If the original image is the color image and if it is not noise affected then the original color image is also degraded with the noise addition process. Different types of noise (GWN, Poisson noise, multiplicative noise, salt and pepper noise) can be added. The *equation (1)* is used to degrade the original image.

$$f_D(x,y) = f_O(x,y) + \eta(x,y) \quad (1)$$

where $f_D(x,y) \rightarrow$ Degraded image with noise insertion, $f_O(x,y) \rightarrow$ Original color or grey level image without noise, $\eta(x,y) \rightarrow$ Inserted noise from the selected noise types. In this presented work, different variance values (0.01 to 0.05) are used to add GWN.

### 2.2 Image Decomposition Approach

The input image (degraded image or noise affected image) $f_D(x,y)$ is decomposed into three components $f_{D_1}(x,y)$, $f_{D_2}(x,y)$, and $f_{D_3}(x,y)$ which have the same resolution as that of the input image. Block schematic of the decomposition process and general process of different component formation is shown in *figure 1*. *Figure 1 (a)* illustrates the degraded image decomposition in three components using the average filter *F*.

FOREX Publication
Open Access | Rapid and quality publishing
International Journal of Electrical and Electronics Research (IJEER)
Research Article | Volume 12, Special Issue -BDF| Pages 19-27 | e-ISSN: 2347-470X

General process of different component formation is depicted in *figure 1 (b)* through *figure 1 (f)*.

### 2.2.1. Componenet-1 Formation

The procedure adopted in the decomposition of the degraded image in componenet-1 is shown in *figure 1 (b)* where the filtering of the degraded image is carried out by using average filter. *Equation (2)* is used for the formation of componenet-1.

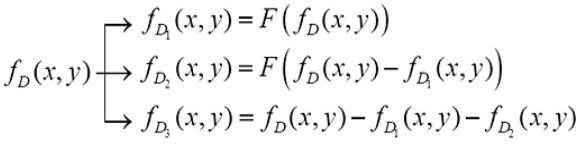


(a)

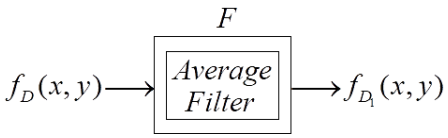


(b)

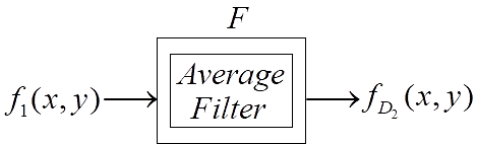


(c)

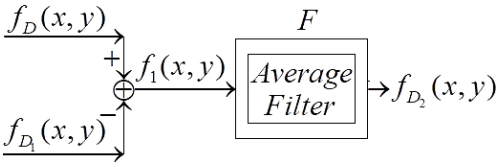


(d)

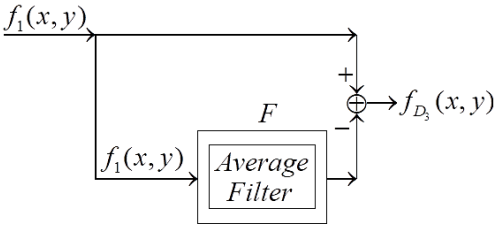


(e)

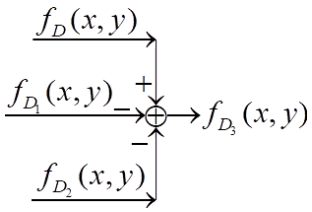


(f)

**Figure 1.** (a) Block schematic of the decomposition process; (b) Component-1; (c) and (d) Component-2; (e) and (f) Component-3

$$f_{D_1}(x,y) = F(f_D(x,y)) \quad (2)$$

The process adopted for the formation of component-1 is as follows.

*Step-1:* Refer the original grey level or color image.
*Step-2:* If an input image is already noise affected then go to *step-4* else perform *step-3*.
*Step-3:* Add the noise from the noise set to the original grey level or color image to get the degraded image.
*Step-4:* If the degraded image is the color image, then perform Step-5 else go to Step-6.
*Step-5:* Separate three grey level planes (i.e., *R*, *G* and *B*) from the degraded color image.
*Step-6:* Filter the degraded grey level image using average filter to get component-1.

### 2.2.2. Componenet-2 Formation

The procedure adopted in the decomposition of the degraded image in componenet-2 is depicted in *figure 1 (c)* and *figure 1 (d)* where the filtering of the degraded image is carried out by using average filter. The *equation (3)* is used for the formation of componenet-2.

$$f_{D_2}(x,y) = F(f_1(x,y)) \quad (3)$$

where $f_1(x,y) = f_D(x,y) - f_{D_1}(x,y)$.

The process adopted for the formation of component-2 is as follows.

*Step-1:* Refer the process of Component-1 formation to get component-1.
*Step-2:* Subtract the Component-1 image from the degraded grey level image to get the intermediate image $f_1(x,y)$.
*Step-3:* Filter the intermediate image $f_1(x,y)$ using average filter to get component-2.

### 2.2.3. Componenet-3 Formation

The procedure adopted in the decomposition of the degraded image in componenet-3 is shown in *figure 1 (e)* and *figure 1 (f)* where the filtering of the degraded image is carried out by using average filter. The *equation (4)* through *equation (6)* are used for the formation of componenet-3.

$$f_{D_3}(x,y) = f_1(x,y) - F(f_1(x,y)) \quad (4)$$

As $f_1(x,y) = f_D(x,y) - f_{D_1}(x,y)$, therefore,

$$f_{D_3}(x,y) = f_D(x,y) - f_{D_1}(x,y) - F(f_1(x,y)) \quad (5)$$

As $f_{D_2}(x,y) = F(f_1(x,y))$, therefore,

$$f_{D_3}(x,y) = f_D(x,y) - f_{D_1}(x,y) - f_{D_2}(x,y) \quad (6)$$

FOREX Publication
Open Access | Rapid and quality publishing
International Journal of Electrical and Electronics Research (IJEER)
Research Article | Volume 12, Special Issue -BDF| Pages 19-27 | e-ISSN: 2347-470X

The process adopted for the formation of component-3 is as follows.

*Step-1:* Refer the process of component-1 formation to get component-1.
*Step-2:* Subtract the component-1 image from the degraded grey level image to get the intermediate image $f_1(x, y)$.
*Step-3:* Refer the process of component-2 formation to get component-2.
*Step-4:* Subtract the component-2 image from the intermediate image $f_1(x, y)$ (*i.e.*, Subtract the component-2 image and component-1 image from the degraded grey level image).

### 2.3 Image Restoration Approach

In view of the restoration of the original grey level image or color image, once again the average and median filters are used. Once three image components, namely, $f_{D_1}(x, y)$, $f_{D_2}(x, y)$, and $f_{D_3}(x, y)$ are obtained, then the filtering (average filter and median filter) is applied on the obtained three components to get independent three filtered images. Later, these three filtered images are combined to get the respective reconstructed grey level plane images. Finally, reconstructed grey level plane images are combined to get the reconstructed color image. The process for the restoration of the color image is as follows.

*Step-1:* Select the filter for restoration.
*Step-2:* Perform the *step-3* through *step-7* for each grey level plane of the color image.
*Step-3:* Refer obtained decomposed components for the respective grey level plane.
*Step-4:* Perform filtering of component-1 using selected filter to get the filtered image for component-1.
*Step-5:* Perform filtering of component-2 using selected filter to get the filtered image for component-2.
*Step-6:* Perform filtering of component-3 using selected filter to get the filtered image for component-3.
*Step-7:* Combine the obtained results of *step-4* through *step-6* to get the reconstructed image of the respective grey level plane.
*Step-8:* Evaluate the reconstructed grey level planes against the original grey level planes using identified performance evaluation parameters.
*Step-9:* Combine the obtained results of *step-7* for each grey level planes to get reconstructed color image.

## 3. EXPERIMENTAL SETUP AND RESULTS

Experiments are performed on the standard image dataset [33] with the System Specifications: Processor: i3-2350 M, 2.30 GHz, 4 Logical Processor(s), 2 Core(s), x64-based PC. To apply the proposed filtering-based image decomposition and restoration approach, the grey level or color images are degraded with the 0.01 to 0.05 variance GWN. Selected original color images (Aeroplane, House, Lena, Mandrill, Sailboat and Splash) of size 256 × 256 are used to carry out experiments.

Obtained results for different color images with selected noise variance values are shown in *figure 2* through *figure 8*. *Table 1* summarizes the results associated with the performance evaluation parameters. *Figure 2 (a)* through *figure 2 (b)* show the results which are obtained with the 0.01 and 0.02 variance Gaussian white noise for the Aeroplane and House color images, respectively. *Figure 3 (a)* and *figure 3 (b)* shows the results which are obtained with the 0.03 and 0.01 variance Gaussian white noise for the Lena and Mandrill color images, respectively. *Figure 4 (a)* and *figure 4 (b)* show the results which are obtained with the 0.04 and 0.05 variance Gaussian white noise for the Sailboat and Splash color images, respectively. From *figure 1 (a)* and *figure 2* through *figure 4*, the following observations are drawn. Component-1 consist of around all details of the image with smaller noise, component-2 consist of smaller noise with missing details of component-1 and component-3 consist of the majority of noise along with the remaining details of the image.

Obtained results of image decomposition are used for the image restoration purpose. Though there are different approaches exist for the image restoration, simple average and median filters are used in presented image restoration approach to reconstruct the color images. *Figure 5* and *figure 6* show the results for the use of average filter to reconstruct the grey level planes and color images along with self-similarity index measure maps (SSIM).

*Figure 5 (a)* shows the results for the reconstructed color images of Aeroplane, House and Lena with the noise variances 0.01, 0.02 and 0.03, respectively. *Figure 5 (b)* shows the result of reconstructed grey level planes of Aeroplane, House and Lena color images and *figure 5 (c)* shows the SSIM maps for the reconstructed grey level planes and the original grey level planes of Aeroplane, House and Lena color images. *Figure 6 (a)* shows the results for the reconstructed color images of Mandrill, Sailboat and Splash with the noise variances 0.01, 0.04 and 0.05, respectively. *Figure 6 (b)* shows the result of reconstructed grey level planes of Mandrill, Sailboat and Splash color images and *figure 6 (c)* shows the SSIM maps for the reconstructed grey level planes and original grey level planes of Mandrill, Sailboat and Splash color images.

Likewise, *figure 7* and *figure 8* show the results for the use of median filter to reconstruct the grey level planes and color images along with SSIM maps for the Aeroplane, House, Lena, Mandrill, Sailboat and Splash color images with the noise variances 0.01, 0.02, 0.03, 0.04 and 0.05, respectively. Obtained results for image restoration using average and median filters are summarized in *table 1*.

Performance evaluation parameters used for comparison of obtained results are- MSE (Mean Squared Error), PSNR (Peak Signal to Noise Ratio), SNR (Signal to Noise Ratio), SSIM (Structural Similarity Index Measure), CC (Correlation Coefficient).

FOREX Publication
Open Access | Rapid and quality publishing
International Journal of
Electrical and Electronics Research (IJEER)
Research Article | Volume 12, Special Issue -BDF| Pages 19-27 | e-ISSN: 2347-470X

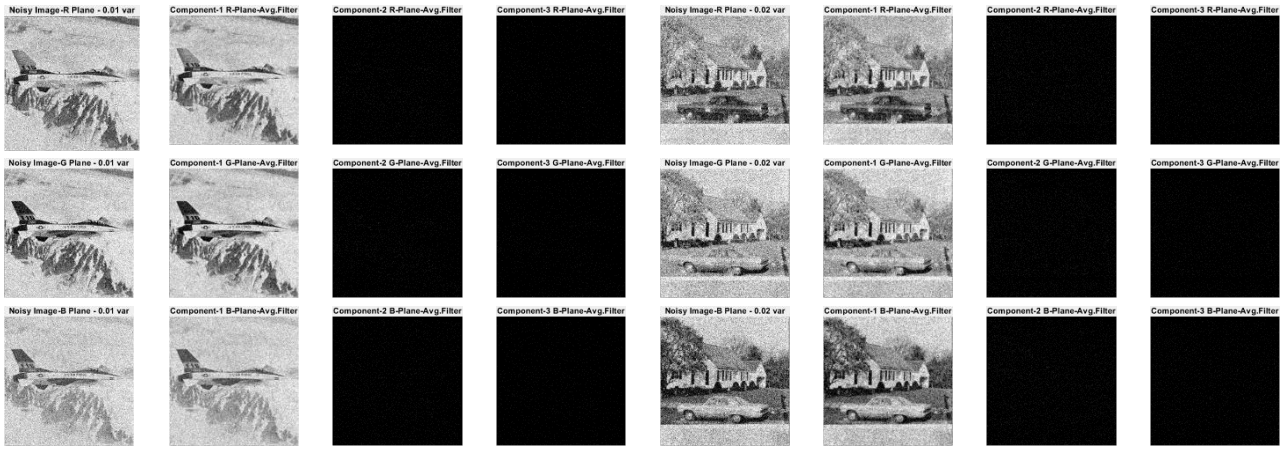


(a) (b)

**Figure 2.** Decomposed components of R, G, and B planes (a) Aeroplane color image (0.01 noise variance); (b) House color image (0.02 noise variance).

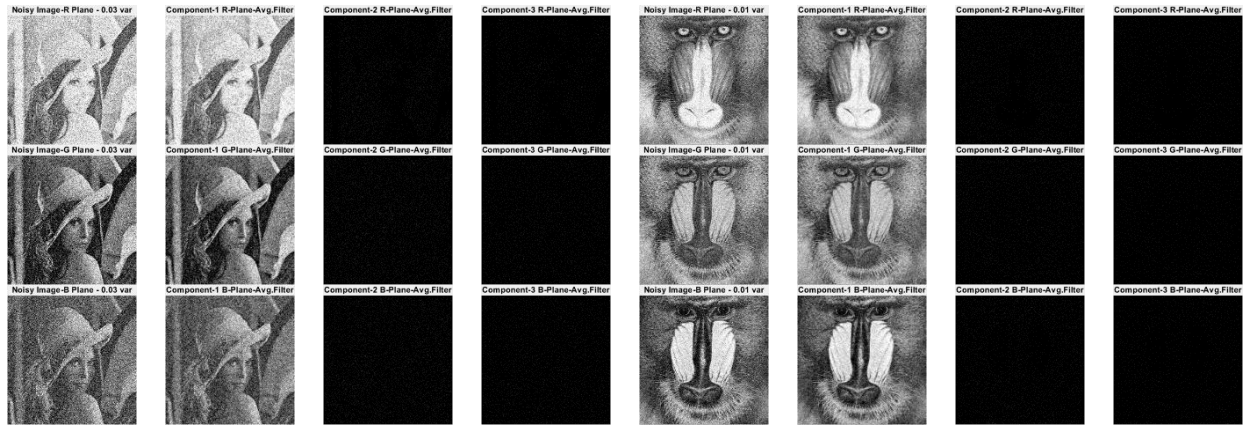


(a) (b)

**Figure 3.** Decomposed components of R, G, and B planes (a) Lena color image (0.03 noise variance); (b) Mandrill color image (0.01 noise variance).

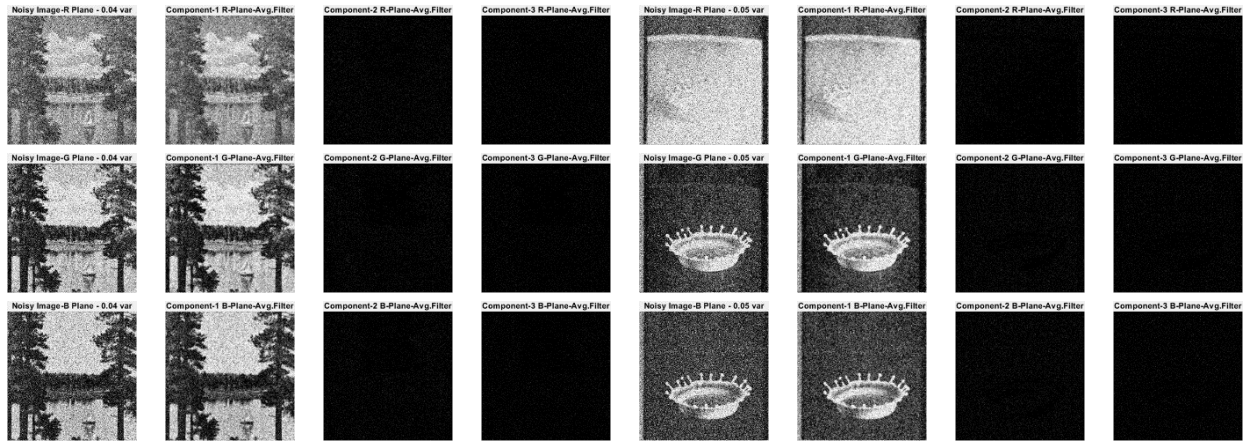


(a) (b)

**Figure 4.** Decomposed components of R, G, and B planes (a) Sailboat color image (0.04 noise variance); (b) Splash color image (0.05 noise variance).

FOREX Publication
Open Access | Rapid and quality publishing
International Journal of
Electrical and Electronics Research (IJEER)
Research Article | Volume 12, Special Issue -BDF| Pages 19-27 | e-ISSN: 2347-470X

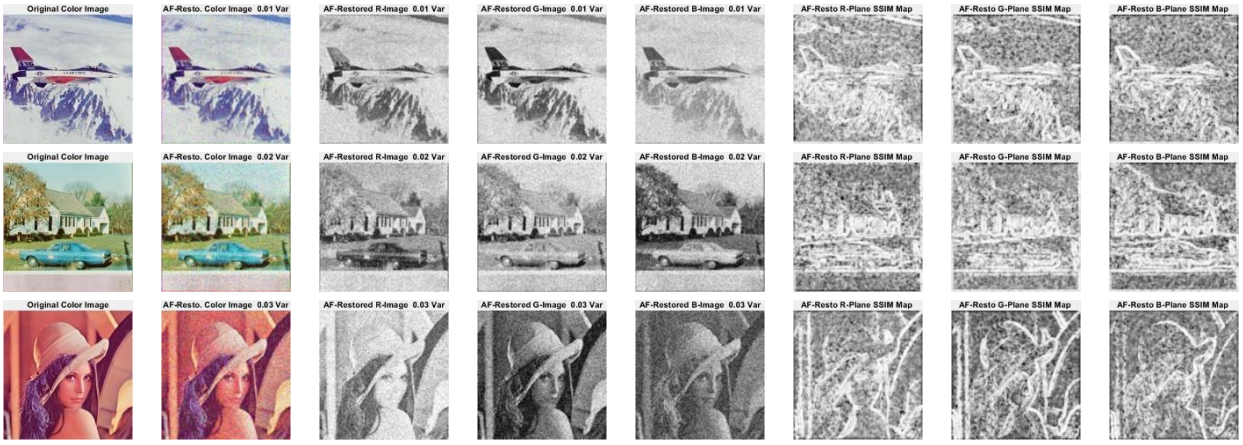


(a) (b) (c)

**Figure 5.** Image restoration results using average filter for Aeroplane, House and Lena color images (a) Original and reconstructed color images; (b) Reconstructed grey level planes; (c) SSIM map images for grey level planes.

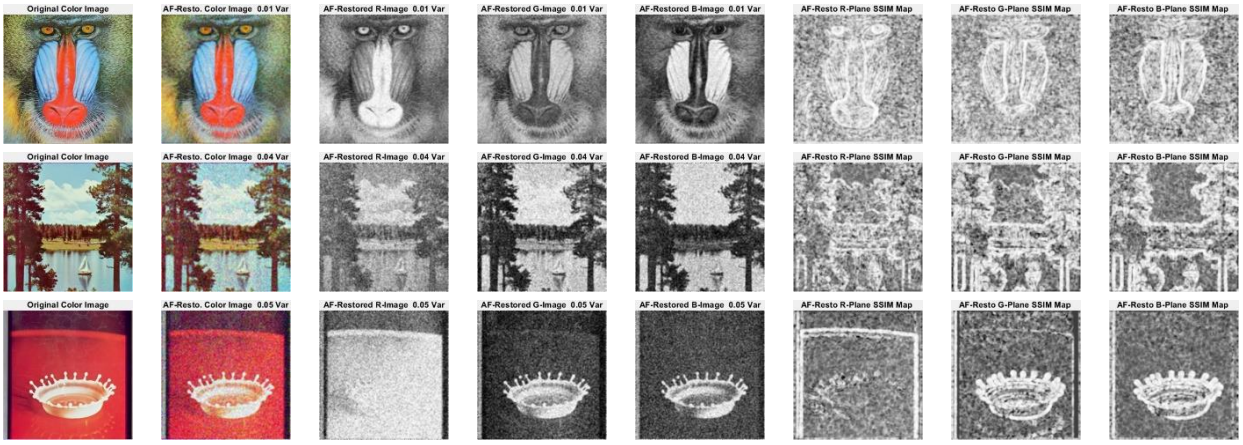


(a) (b) (c)

**Figure 6.** Image restoration results using average filter for Mandrill, Sailboat and Splash color images (a) Original and reconstructed color images; (b) Reconstructed grey level planes; (c) SSIM map images for grey level planes.

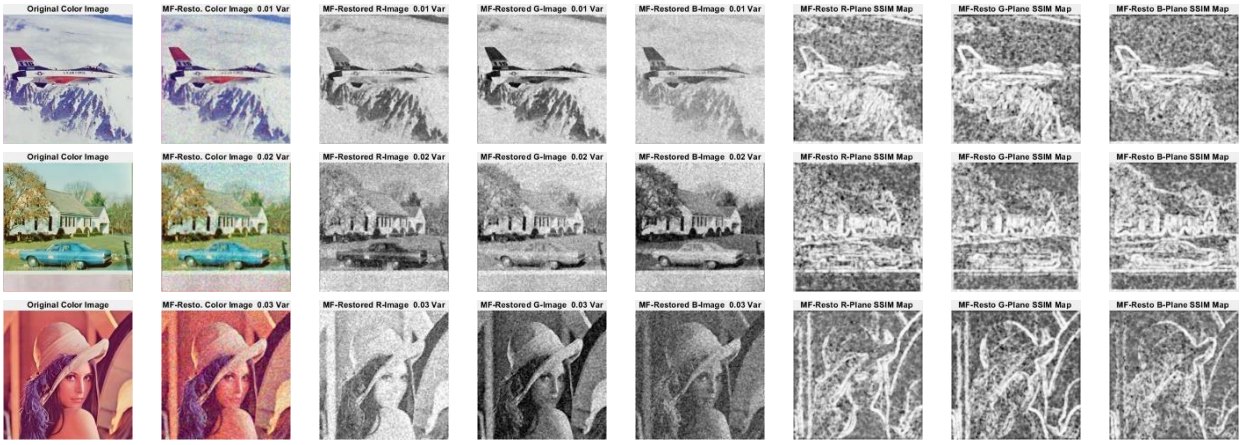


(a) (b) (c)

**Figure 7.** Image restoration results using median filter for Aeroplane, House and Lena color images (a) Original and reconstructed color images; (b) Reconstructed grey level planes; (c) SSIM map images for grey level planes.

FOREX Publication
Open Access | Rapid and quality publishing
International Journal of Electrical and Electronics Research (IJEER)
Research Article | Volume 12, Special Issue -BDF| Pages 19-27 | e-ISSN: 2347-470X

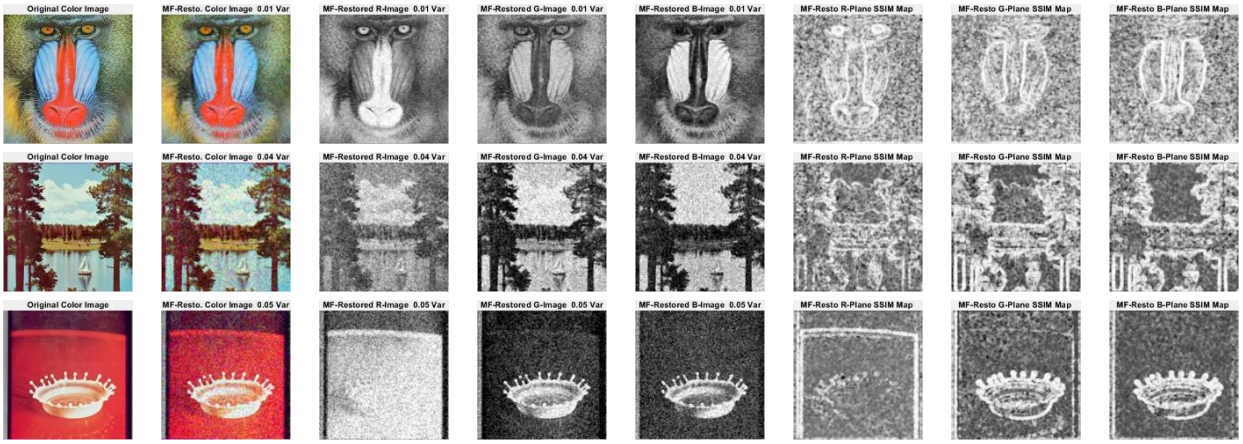


(a) (b) (c)

**Figure 8.** Image restoration results using median filter for Mandrill, Sailboat and Splash color images (a) Original and reconstructed color images; (b) Reconstructed grey level planes; (c) SSIM map images for grey level planes.

**Table 1. Summary of obtained results for image restoration using average and median filters**

| Image | | Average Filter Results | | | | | | Median Filter Results | | | | |
|---|---|---|---|---|---|---|---|---|---|---|---|---|
| | P | NV | MSE | PSNR | SNR | SSIM | CC | MSE | PSNR | SNR | SSIM | CC |
| Aeroplane | R | 0.01 | 189.48 | 25.36 | 22.47 | 0.69 | 0.96 | 179.71 | 25.58 | 22.70 | 0.64 | 0.95 |
| | G | 0.01 | 218.66 | 24.73 | 21.95 | 0.69 | 0.96 | 201.16 | 25.10 | 22.31 | 0.64 | 0.96 |
| | B | 0.01 | 145.78 | 26.49 | 24.06 | 0.65 | 0.94 | 144.23 | 26.54 | 24.11 | 0.59 | 0.93 |
| House | R | 0.02 | 313.10 | 23.17 | 19.29 | 0.60 | 0.94 | 323.64 | 23.03 | 19.15 | 0.54 | 0.93 |
| | G | 0.02 | 324.87 | 23.01 | 19.73 | 0.60 | 0.94 | 330.03 | 22.95 | 19.66 | 0.55 | 0.93 |
| | B | 0.02 | 308.93 | 23.23 | 18.88 | 0.62 | 0.96 | 308.23 | 23.24 | 18.89 | 0.57 | 0.96 |
| Lena | R | 0.03 | 285.64 | 23.57 | 20.87 | 0.54 | 0.95 | 333.57 | 22.90 | 20.19 | 0.46 | 0.93 |
| | G | 0.03 | 385.07 | 22.28 | 15.13 | 0.53 | 0.95 | 371.99 | 22.43 | 15.28 | 0.47 | 0.94 |
| | B | 0.03 | 350.25 | 22.69 | 15.43 | 0.47 | 0.88 | 352.40 | 22.66 | 15.40 | 0.41 | 0.86 |
| Mandrill | R | 0.01 | 254.76 | 24.07 | 19.29 | 0.63 | 0.96 | 252.15 | 24.11 | 19.34 | 0.60 | 0.95 |
| | G | 0.01 | 344.39 | 22.76 | 17.29 | 0.60 | 0.92 | 332.43 | 22.91 | 17.45 | 0.58 | 0.91 |
| | B | 0.01 | 343.28 | 22.77 | 16.74 | 0.62 | 0.95 | 329.64 | 22.95 | 16.91 | 0.59 | 0.95 |
| Sailboat | R | 0.04 | 433.77 | 21.76 | 16.40 | 0.48 | 0.91 | 464.12 | 21.46 | 16.10 | 0.41 | 0.88 |
| | G | 0.04 | 546.62 | 20.75 | 15.91 | 0.56 | 0.96 | 564.13 | 20.62 | 15.77 | 0.51 | 0.95 |
| | B | 0.04 | 507.66 | 21.08 | 15.72 | 0.52 | 0.96 | 523.09 | 20.95 | 15.59 | 0.46 | 0.96 |
| Splash | R | 0.05 | 353.18 | 22.65 | 19.91 | 0.41 | 0.95 | 456.10 | 21.54 | 18.80 | 0.31 | 0.94 |
| | G | 0.05 | 572.07 | 20.56 | 11.75 | 0.37 | 0.94 | 501.15 | 21.13 | 12.32 | 0.33 | 0.93 |
| | B | 0.05 | 527.17 | 20.91 | 12.09 | 0.36 | 0.91 | 533.11 | 20.86 | 12.04 | 0.30 | 0.89 |

*(P-Image Plane, NV- Noise variance)*

## 4. DISCUSSION

With reference to image decomposition approach various values of variances, *i.e.*, 0.01, 0.02, 0.03, 0.04, and 0.05 are used for the insertion of Gaussian white noise with zero mean in the three grey level planes of color images. Inserted noise and the image details are distributed in three decomposed components of the grey level planes. Component-1 consists of the majority of image details while the majority of noise is present in the component-3. Component-2 consists of less noise along with the missing details of component-1. Requirement of execution time for the image decomposition is very less. In general, the linear and non-linear filters are used for the image restoration. In this paper, the smallest window size of 3 × 3 is used for the image decomposition and restoration. From obtained results of the image restoration, it is clear that the reconstructed image quality is degrading as the noise variance value increases. Some sample results are discussed in this paper. It is clear from the *table 1* that the SNR values are better for the Aeroplane and Mandrill images when the restoration results are obtained by median filter and it is due to the fine details available in

Aeroplane and Mandrill images. While the SNR values are better for the House, Lena Sailboat and Splash images when the restoration results are obtained by average filter.

## 5. CONCLUSION AND FUTURE SCOPE

The lightweight image decomposition approach is proposed in this paper which can be easily incorporated for the different sort of processing of images. For example, the image compression approach can be developed using presented image decomposition approach. Image restoration is carried out on the decomposed components obtained after the application of decomposition approach with the linear filter (average) and non-linear filter (median). Better results are obtained for images with fine details in the case of non-linear filter and vice-versa.

In the future, the thresholding approach can be used for the restoration or the combination of different filters can be used to improve the results. Variable size windows can be used to decompose and restore the images.

**Conflicts of Interest:** The authors declare no conflict of interest.

## REFERENCES

[1] D. -A. Huang, L. -W. Kang, Y. -C. F. Wang and C. -W. Lin, "Self-Learning Based Image Decomposition with Applications to Single Image Denoising," in IEEE Transactions on Multimedia, vol. 16, no. 1, pp. 83-93, Jan. 2014, doi: 10.1109/TMM.2013.2284759.

[2] X. -Y. Cui, Z. -G. Gui, Q. Zhang, H. Shangguan and A. -H. Wang, "Learning-Based Artifact Removal via Image Decomposition for Low-Dose CT Image Processing," in IEEE Transactions on Nuclear Science, vol. 63, no. 3, pp. 1860-1873, June 2016, doi: 10.1109/TNS.2016.2565604.

[3] J. Du, W. Li and H. Tan, "Intrinsic Image Decomposition-Based Grey and Pseudo-Color Medical Image Fusion," in IEEE Access, vol. 7, pp. 56443-56456, 2019, doi: 10.1109/ACCESS.2019.2900483.

[4] D. Hauagge, S. Wehrwein, K. Bala and N. Snavely, "Photometric Ambient Occlusion for Intrinsic Image Decomposition," in IEEE Transactions on Pattern Analysis and Machine Intelligence, vol. 38, no. 4, pp. 639-651, 1 April 2016, doi: 10.1109/TPAMI.2015.2453959.

[5] X. Kang, S. Li, L. Fang and J. A. Benediktsson, "Intrinsic Image Decomposition for Feature Extraction of Hyperspectral Images," in IEEE Transactions on Geoscience and Remote Sensing, vol. 53, no. 4, pp. 2241-2253, April 2015, doi: 10.1109/TGRS.2014.2358615.

[6] X. Jin and Y. Gu, "Superpixel-Based Intrinsic Image Decomposition of Hyperspectral Images," in IEEE Transactions on Geoscience and Remote Sensing, vol. 55, no. 8, pp. 4285-4295, Aug. 2017, doi: 10.1109/TGRS.2017.2690445.

[7] Kang, X., Li, S., Fang, L. et al. Pansharpening Based on Intrinsic Image Decomposition. Sens Imaging 15, 94 (2014). https://doi.org/10.1007/s11220-014-0094-8

[8] S. Ono, T. Miyata and I. Yamada, "Cartoon-Texture Image Decomposition Using Blockwise Low-Rank Texture Characterization," in IEEE Transactions on Image Processing, vol. 23, no. 3, pp. 1128-1142, March 2014, doi: 10.1109/TIP.2014.2299067.

[9] H. Zhang and V. M. Patel, "Convolutional Sparse and Low-Rank Coding-Based Image Decomposition," in IEEE Transactions on Image Processing, vol. 27, no. 5, pp. 2121-2133, May 2018, doi: 10.1109/TIP.2017.2786469.

[10] Gupta, B., Singh, A. A new computational approach for edge-preserving image decomposition. Multimed Tools Appl 77, 19527–19546 (2018). https://doi.org/10.1007/s11042-017-5401-7

[11] Shao, P., Ding, S., Ma, L. et al. Edge-preserving image decomposition via joint weighted least squares. Comp. Visual Media 1, 37–47 (2015). https://doi.org/10.1007/s41095-015-0006-4

[12] J. Song, H. Cho, J. Yoon and S. M. Yoon, "Structure Adaptive Total Variation Minimization-Based Image Decomposition," in IEEE Transactions on Circuits and Systems for Video Technology, vol. 28, no. 9, pp. 2164-2176, Sept. 2018, doi: 10.1109/TCSVT.2017.2717542.

[13] L. Jiang and H. Yin, "Fractional-order variational regularization for image decomposition," 2014 19th International Conference on Digital Signal Processing, Hong Kong, China, 2014, pp. 24-29, doi: 10.1109/ICDSP.2014.6900821.

[14] Huang, H., Wang, K. (2017). Texture-preserving deconvolution via image decomposition. Signal, Image and Video Processing, 11(7), 1189–1196. https://doi.org/10.1007/s11760-017-1074-y

[15] Bellamine, I., Tairi, H. Optical flow estimation based on the structure–texture image decomposition. SIViP 9 (Suppl 1), 193–201 (2015). https://doi.org/10.1007/s11760-015-0772-6

[16] T. N. Canh, K. Q. Dinh and B. Jeon, "Detail-preserving compressive sensing recovery based on cartoon texture image decomposition," 2014 IEEE International Conference on Image Processing (ICIP), Paris, France, 2014, pp. 1327-1331, doi: 10.1109/ICIP.2014.7025265.

[17] Qiang, Z., Liu, H., Shang, Z. (2019). Image Inpainting Based on Image Structure and Texture Decomposition. In: Deng, K., Yu, Z., Patnaik, S., Wang, J. (eds) Recent Developments in Mechatronics and Intelligent Robotics. ICMIR 2018. Advances in Intelligent Systems and Computing, vol 856. Springer, Cham. https://doi.org/10.1007/978-3-030-00214-5_134

[18] Yang, J., Lin, Y., Ou, B. et al. Image decomposition-based structural similarity index for image quality assessment. J Image Video Proc. 2016, 31 (2016). https://doi.org/10.1186/s13640-016-0134-5

[19] Zhaodong Liu, Yi Chai, Hongpeng Yin, Jiayi Zhou, Zhiqin Zhu, A novel multi-focus image fusion approach based on image decomposition, Information Fusion, Volume 35, 2017, Pages 102-116, ISSN 1566-2535, https://doi.org/10.1016/j.inffus.2016.09.007.

[20] Jiang, X., Yao, H. & Liu, D. Nighttime image enhancement based on image decomposition. SIViP 13, 189–197 (2019). https://doi.org/10.1007/s11760-018-1345-2

[21] Ling Zhang, Qingan Yan, Yao Zhu, Xiaolong Zhang, and Chunxia Xiao. 2019. Effective shadow removal via multi-scale image decomposition. Vis. Comput. 35, 6–8 (June 2019), 1091–1104. https://doi.org/10.1007/s00371-019-01685-8

[22] Ma, GH., Zhang, ML., Li, XM. et al. Image Smoothing Based on Image Decomposition and Sparse High Frequency Gradient. J. Comput. Sci. Technol. 33, 502–510 (2018). https://doi.org/10.1007/s11390-018-1834-3

[23] Muhammad, N., Bibi, N., Qasim, I. et al. Digital watermarking using Hall property image decomposition method. Pattern Anal Applic 21, 997–1012 (2018). https://doi.org/10.1007/s10044-017-0613-z

[24] Xiaoyu Fan, Qiusheng Lian, Baoshun Shi, Compressed sensing MRI based on image decomposition model and group sparsity, Magnetic Resonance Imaging, Volume 60, 2019, Pages 101-109, ISSN 0730-725X, https://doi.org/10.1016/j.mri.2019.03.011.

[25] Ho-Gun Ha, Wang-Jun Kyung, Ji-Hoon Yoo and Yeong-Ho Ha, "Simultaneous color matching in stereoscopic images based on image decomposition," 2014 IEEE Fourth International Conference on Consumer Electronics Berlin (ICCE-Berlin), Berlin, Germany, 2014, pp. 149-152, doi: 10.1109/ICCE-Berlin.2014.7034216.

[26] Q. Chang and J. Chen, "Fusion of backscatter and transmission images based on multi-scale image decomposition," 2014 International Conference on Audio, Language and Image Processing, Shanghai, China, 2014, pp. 234-238, doi: 10.1109/ICALIP.2014.7009792.

[27] C. Rong, Y. Jia, Y. Yang, Y. Zhu and Y. Wang, "Fusion of Infrared and Visible Images through a Hybrid Image Decomposition and Sparse Representation," 2018 10th International Conference on Intelligent Human-Machine Systems and Cybernetics (IHMSC), Hangzhou, China, 2018, pp. 21-25, doi: 10.1109/IHMSC.2018.10111.

[28] Jamlee Ludes, B., Norman, S.R. (2016). Enhancement of Endoscopic Image Using TV-Image Decomposition. In: Suresh, L., Panigrahi, B. (eds) Proceedings of the International Conference on Soft Computing Systems. Advances in Intelligent Systems and Computing, vol 397. Springer, New Delhi. https://doi.org/10.1007/978-81-322-2671-0_7.

[29] N. V. Thakur and O. G. Kakde, "Fractal Color Image Compression on a Pseudo Spiral Architecture," 2006 IEEE Conference on Cybernetics and Intelligent Systems, Bangkok, Thailand, 2006, pp. 1-6, doi: 10.1109/ICCIS.2006.252295.

[30] S. R. Mahakale and N. V. Thakur, "A Comparative Study of Image Filtering on Various Noisy Pixels", International Journal of Image Processing and Vision Science, vol. 1, no. 3, 2013, doi: 10.47893/IJIPVS.2013.1029.

International Journal of
Electrical and Electronics Research (IJEER)
Research Article | Volume 12, Special Issue -BDF| Pages 19-27 | e-ISSN: 2347-470X

[31] P. Y. Panchbhai and N. V. Thakur, “Performing Multiplications in Image Filtering Process using Vedic Mathematics”, International Journal of Image Processing and Vision Science, vol. 2, no. 1, 2013, doi: 10.47893/IJIPVS.2013.10.
[32] S. D. Kamble, N. V. Thakur, P. R. Bajaj, “A Review on Block Matching Motion Estimation and Automata Theory based Approaches for Fractal Coding”, International Journal of Interactive Multimedia and Artificial Intelligence, vol. 4, no. 2, pp. 91-104, 2016, doi: 10.9781/ijimai.2016.4214.
[33] G. Schaefer and M. Stich (2004) "UCID - An Uncompressed Colour Image Database", Proc. SPIE, Storage and Retrieval Methods and Applications for Multimedia 2004, pp. 472-480, San Jose, USA.